# Study well-shaped germanium detectors for low-background counting

**W.-Z. Wei[1], D.-M. Mei[1,2] and C. Zhang[1]**

[1]Department of Physics, The University of South Dakota, Vermillion, SD 57069, United States
[2]School of Physics and Optoelectronic, Yangtze University, Jingzhou 434023, China

E-mail: Dongming.Mei@usd.edu

**Abstract.** Radiogenic particles are known as the main sources of background for all ultra-low background experiments in the detection of dark matter and neutrino properties. In particular, the radiogenic gamma rays from PMTs are a main component of the observed backgrounds in the noble liquid detectors such as XENON100 and LUX. This suggests a more accurate screening of PMTs is needed for the next generation experiments such as LUX-Zplin or Xenon1T. Hence, we propose to develop well-shaped germanium detectors for a better understanding of the radiogenic background from PMTs. A well-shaped germanium detector array and PMT (R11410MOD) have been designed in a Geant4-based Monte Carlo simulation, in which three radiogenic background isotopes from $^{238}$U, $^{232}$Th and $^{40}$K have been studied. In this work, we show the detector performance including the detector efficiency, energy resolution and the detector sensitivity for low-background counting in the detection of rare event physics.

## 1. Introduction

Radiogenic background plays a critical role in a variety of ultra-low background experiments conducted deep underground for the detection of dark matter and neutrino properties, as radiogenic particles are known to be the main sources of background in those experiments. For example, radiogenic neutrons can cause isolated recoils of atomic nuclei that are indistinguishable from the expected signal of Weekly Interacting Massive Particles (WIMPs), the most promising candidate of dark matter.

Dark matter experiments using noble liquid xenon as detector material, such as XENON100 and LUX, typically employ photomultiplier tubes (PMTs) to detect the scintillation light from the xenon nuclear recoils [1]. PMTs are usually mounted directly above and below the active scintillation region for better detection of photon signals in the scintillation detector [1]. Hence, much attention needs to be paid on the radiogenic background generated from PMTs to maintain low background around the xenon detectors. This necessitates a good understanding of the radioactivity in PMTs, so that the PMTs selected for ultra-low background experiments will be comprised of radiopure materials [1]. In particular, the rediogenic gamma rays from PMTs are a main component of the observed backgrounds in XENON100 [2] and LUX [3], with an observed background rate often higher than what was predicted [2, 3]. This suggests a more accurate screening of PMTs is needed for the next generation experiments such as LUX-Zeplin [4] or Xeonon1T [5] in achieving the target sensitivity for dark matter searches.
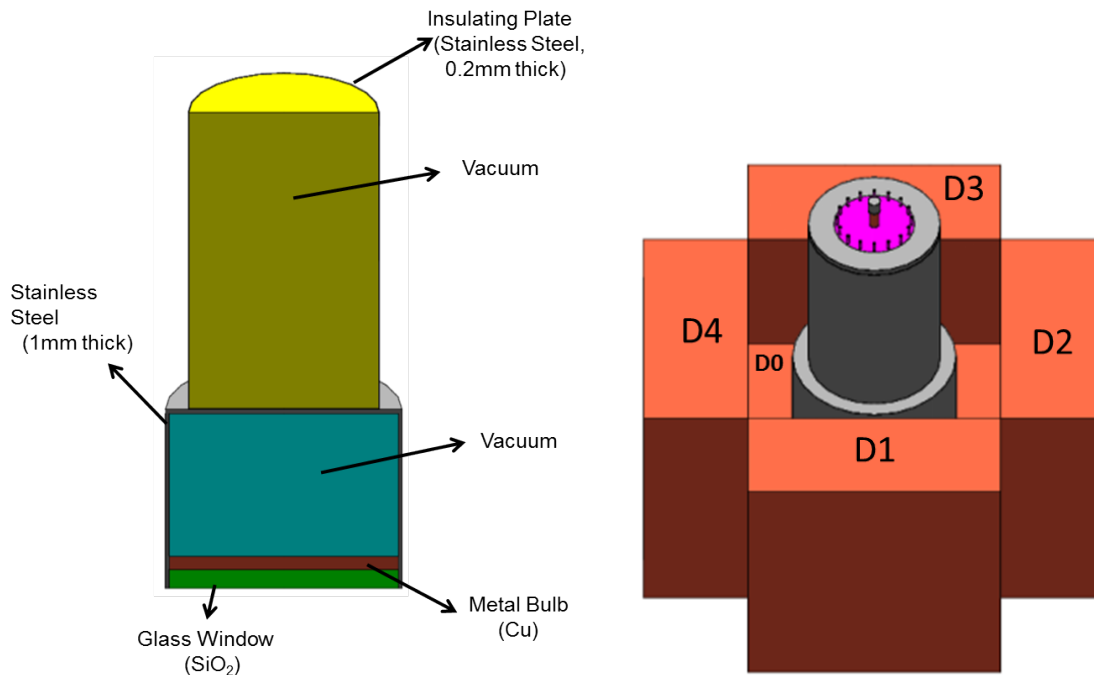
**Figure 1.** Simulated geometry for Ge well detector array and R11410MOD PMT. Left: Cross section of R11410MOD PMT without the lid. Right: Ge well detector array with the PMT in the center of the well, where D0 ∼ D4 represent the corresponding Ge planar detector.

## 2. Monte Carlo simulation set-up

### 2.1. Geometry and material

The proposed Ge well detector was constructed by making five Ge planar detectors in a well shape. Each Ge crystal is about 2.13 kg in mass with the dimension of 10 cm × 10 cm × 4 cm; and each single crystal is inside a very thin Oxygen-Free High-Conducting (OFHC) copper box with 2 mm in thickness. Furthermore, a R11410MOD PMT with dimensions and materials provided in Ref. [6] was simulated as well to provide the signal for the germanium well detector array in order to test how well this detector array will see the signals from PMT. Fig. 1 shows the geometry simulated in the Monte Carlo.

### 2.2. Generator

Three radiogenic isotopes, $^{238}U$, $^{232}Th$ and $^{40}K$, have been generated in the simulation. These three isotopes are prominent contaminants in the PMT and OFHC copper and they are all radioactive and will emit alpha and beta particles in their decay chains. To study the detector performance mentioned in the introduction, we have designed two independent simulations:

(I). Generate $^{238}U$, $^{232}Th$ and $^{40}K$ only in the PMT to study the detector response to the signal from the PMT. $^{238}U$, $^{232}Th$ and $^{40}K$ are distributed uniformly in each component material of the PMT which consists of copper, stainless steel, glass and ceramic. The simulated decays of each isotope in different material of the PMT is proportional to the mass of material, as shown in table 1. Four independent sub-simulations corresponding to four component materials have been conducted for each isotope and then combine them together to study the detector efficiency for a series of gamma rays of interest from those three sources. The detector efficiency will show how well the detector will respond to the signal.

(II). Generate $^{238}U$, $^{232}Th$ and $^{40}K$ only in the five copper boxes to study the detector

**Table 1.** The simulated radioactive decays of each source in different materials of PMT. The total mass of PMT is $\sim$202 g. $10^7$ is the total decays simulated for each source.

| Material | Mass (g) | Mass Percentage (%) | Simulated Decays |
|---|---|---|---|
| Copper | 96.18 | 47.74 | $10^7 \times 47.74\% = 4.774 \times 10^6$ |
| Stainless Steel | 63.23 | 30.89 | $10^7 \times 30.89\% = 3.089 \times 10^6$ |
| Glass | 35 | 17.37 | $10^7 \times 17.37\% = 1.737 \times 10^6$ |
| Ceramic | 8.06 | 4 | $10^7 \times 4\% = 4.0 \times 10^5$ |

response to the background from the shield, copper box. $^{238}U$, $^{232}Th$ and $^{40}K$ are uniformly distributed in the copper box. To obtained how many decays should be simulated for each isotope in the OFHC copper box, two factors are considered when normalizing to simulated decays in the PMT. One is the mass of PMT and copper box. The other is the activity of each isotope in the PMT and OFHC copper. The activity of each isotope in the PMT is assumed to be $\sim$0.01 ppb, which corresponds to 124 $\mu$Bq/kg for $^{238}U$, 40.5 $\mu$Bq/kg for $^{232}Th$ and 2500 $\mu$Bq/kg for $^{40}K$, respectively. The activity of each isotope in the OFHC copper was obtained in Ref [7]. Table 2 shows the simulated decays in the copper box for each isotope.

**Table 2.** The number of decays simulated for each isotope in the copper box. Where, 8.2 in column 5 is the mass ratio between the copper box (1656 g) and PMT (202 g).

| Isotopes | Activity in the PMT ($\mu$Bq/kg) | Activity in the OFHC copper ($\mu$Bq/kg) | Simulated decays in the PMT | Simulated decays in the copper box |
|---|---|---|---|---|
| $^{238}U$ | 124 | 16 | $10^7$ | $10^7 \times \frac{16}{124} \times 8.2 = 4.058 \times 10^7$ |
| $^{232}Th$ | 40.5 | 19 | $10^7$ | $10^7 \times \frac{19}{40.5} \times 8.2 = 3.85 \times 10^7$ |
| $^{40}K$ | 2500 | 88 | $10^7$ | $10^7 \times \frac{88}{2500} \times 8.2 = 2.886 \times 10^6$ |

## 3. Monte Carlo analysis

### 3.1. Detection Efficiency

The basic definition of detection efficiency for photon can be expressed as follows [8]:

$$\varepsilon = \frac{total\ number\ of\ detected\ photons\ in\ the\ full\text{-}energy\ peak}{total\ number\ of\ photons\ emitted\ by\ the\ source} \qquad (1)$$

Where, *total number of photons emitted by the source* is the product of the total decays (*10 million/number of radionuclide in the decay chain of* $^{238}U$, $^{232}Th$ *or* $^{40}K$) and the branching ratio for the photon of interest. The Compton background continuum was taken into account when counting the *total number of detected photons in the full-energy peak* since Compton events are the primary source of background counts under the full-energy peak [8].

Two types of detector efficiency have been studied in simulation I: (1) the five individual detector efficiency ($\varepsilon_{D0}$, $\varepsilon_{D1}$, $\varepsilon_{D2}$, $\varepsilon_{D3}$, and $\varepsilon_{D4}$), and (2) the total detector efficiency from the sum of energy deposition in five individual detectors ($\varepsilon_{total}$). Note that the detection threshold was assumed to be 10 keV for the well-shaped Ge detector array.

Table 3, table 4 and table 5 show the simulation results of these three types of detector efficiencies for each selected gamma ray of interest from the decay chain of $^{238}U$, $^{232}Th$ and $^{40}K$, respectively.

**Table 3.** Detector efficiency for each selected gamma ray of interest from $^{238}U$ decay chain.

| Radionuclide | $E_\gamma$ (keV) | Branching ratio [9] | $\varepsilon_{D0}$ (%) | $\varepsilon_{D1}$ (%) | $\varepsilon_{D2}$ (%) | $\varepsilon_{D3}$ (%) | $\varepsilon_{D4}$ (%) | $\varepsilon_{total}$ (%) |
|---|---|---|---|---|---|---|---|---|
| $^{234}Th$ | 92 | 0.025 | 5.4 | 1.58 | 1.55 | 1.40 | 1.64 | 11.4 |
| $^{234}Pa$ | 1001 | 0.0056 | 11.3 | 2.54 | 2.44 | 2.57 | 2.52 | 24.3 |
| $^{226}Ra$ | 186 | 0.035 | 15.2 | 4.22 | 4.24 | 4.08 | 4.39 | 28.6 |
| $^{214}Pb$ | 352 | 0.342 | 12.0 | 3.15 | 3.00 | 3.09 | 3.13 | 26.6 |
| | 295 | 0.177 | 12.7 | 3.36 | 3.24 | 3.25 | 3.21 | 27.9 |
| $^{214}Bi$ | 2204 | 0.046 | 4.11 | 1.17 | 1.20 | 1.10 | 1.20 | 11.3 |
| | 1847 | 0.002 | 5.60 | 1.31 | 1.35 | 1.41 | 1.26 | 19.5 |
| | 1764 | 0.147 | 4.53 | 1.25 | 1.29 | 1.19 | 1.21 | 12.2 |
| | 1120 | 0.141 | 4.08 | 1.47 | 1.41 | 1.49 | 1.51 | 6.46 |

**Table 4.** Detector efficiency for each selected gamma ray of interest from $^{232}Th$ decay chain.

| Radionuclide | $E_\gamma$ (keV) | Branching ratio [10] | $\varepsilon_{D0}$ (%) | $\varepsilon_{D1}$ (%) | $\varepsilon_{D2}$ (%) | $\varepsilon_{D3}$ (%) | $\varepsilon_{D4}$ (%) | $\varepsilon_{total}$ (%) |
|---|---|---|---|---|---|---|---|---|
| $^{228}Ac$ | 969 | 0.162 | 5.56 | 1.61 | 1.64 | 1.60 | 1.57 | 13.4 |
| | 911 | 0.266 | 5.87 | 1.64 | 1.63 | 1.59 | 1.61 | 13.9 |
| | 338 | 0.113 | 11.7 | 3.20 | 3.25 | 3.23 | 3.20 | 24.0 |
| $^{228}Th$ | 84.4 | 0.013 | 4.83 | 0.982 | 0.99 | 1.05 | 1.02 | 9.08 |
| $^{224}Ra$ | 241 | 0.004 | 13.6 | 3.36 | 3.36 | 3.12 | 3.45 | 28.2 |
| $^{212}Pb$ | 239 | 0.436 | 13.2 | 3.39 | 3.35 | 3.37 | 3.39 | 28.1 |
| $^{212}Bi$ | 727 | 0.067 | 7.03 | 2.13 | 2.04 | 2.08 | 1.98 | 15.5 |
| $^{208}Ti$ | 583 | 0.304 | 5.44 | 1.96 | 1.92 | 1.91 | 1.95 | 8.22 |

**Table 5.** Detector efficiency for each selected gamma ray of interest from $^{232}Th$ decay chain.

| Radionuclide | $E_\gamma$ (keV) | Branching ratio | $\varepsilon_{D0}$ (%) | $\varepsilon_{D1}$ (%) | $\varepsilon_{D2}$ (%) | $\varepsilon_{D3}$ (%) | $\varepsilon_{D4}$ (%) | $\varepsilon_{total}$ (%) |
|---|---|---|---|---|---|---|---|---|
| $^{40}K$ | 1461 | 0.105 | 4.63 | 1.25 | 1.23 | 1.26 | 1.25 | 12.10 |

The results of simulation I are summarized in tables 3 - 5, which show that the Ge planar detector, D0 (at the bottom of the well), is most sensitive to the signal from the PMT,

indicating that the individual detector efficiency has a strong position dependence. This property can be used to track gamma rays from the PMT and other detector components for a better understanding of the backgrounds. Moreover, due to the well-shaped geometry, the total detector efficiency of the proposed detector array for low-energy $\gamma$-rays has a factor of $\sim 2$ improvement when comparing to that of the single planar Ge detector with best detector efficiency.

### 3.2. Minimum detectable activity (MDA)

In addition to the detector efficiency, we have also studied another detector performance, Minimum Detectable Activity (MDA) in simulation II.

The Minimum Detectable Activity (MDA) is defined as the smallest amount of radioactivity that can be distinguished from a blank sample. When the count rate of a sample is roughly the same as the count rate of the background, the MDA becomes significant in low-level counting. The MDA for $\gamma$-ray measurement system can be calculated according to the equation [11] below:

$$MDA = \frac{\alpha \sqrt{N_b}}{r_b \Delta T \varepsilon M} \qquad (2)$$

Where, $MDA$ is in Bq/kg or Bq/PMT, $\alpha$ is a constant that equals to 1.64 at 90% confidence level (C.L.), $N_b$ is the number of background counts in the region of interest (ROI) for a $\gamma$ ray from a target redionuclide, $r_b$ is the branching ratio of the selected $\gamma$ ray from the target radionuclide, $\Delta T$ is the counting time in seconds, $\varepsilon$ is the full absorption efficiency for the selected $\gamma$ ray, and $M$ is the mass of the counting sample, which is the PMT ( 201.47 g) in our work.

$r_b$ and $\varepsilon$ can be directly obtained from simulation I (table $3 \sim 5$ ). $\Delta T$ can be calculated from the given total simulated decays and activity in OFHC copper for each isotope, which are $2.66 \times 10^{10} s$ ($4.4 \times 10^4$ weeks), $1.11 \times 10^{11} s$ ($1.84 \times 10^5$ weeks), and $1.98 \times 10^{10} s$ ($3.27 \times 10^4$ weeks) for $^{238}U$, $^{232}Th$ and $^{40}K$, respectively. Hence, the only parameter needs to be determined in Eq. 2 is $N_b$, the number of backgrounds counts in the ROI, to calculate the $MDA$ for each selected gamma ray from the decay chain of $^{238}U$, $^{232}Th$ and $^{40}K$. The energy resolution for each selected gamma ray needs to be taken into account in order to get the corresponding background counts, $N_b$, from simulation II. 12 gamma rays and their corresponding Full Width at Half Maximum (HWHM) from Ref. [12] were used to fit the energy resolution. The best fit function is presented in Eq. 3:

$$FWHM = (1.423 \pm 0.019) + (6.168 \pm 0.639) \times 10^{-5} \cdot E_r - (6.475 \pm 4.391) \times 10^{-8} \cdot E_r^2 \quad (3)$$

Where, $E_r$ is the energy of the selected $\gamma$ ray. The energy resolution in terms of FWHM as a function of the $\gamma$ ray energy is plotted in Fig. 2.

With Eq. 3, the $FWHM$ and thus the $MDA$ of each selected gamma ray can then be calculated.

Table 6, table 7 and table 8 show the simulation results of $FWHM$ and $MDA$ for each selected gamma rays from $^{238}U$, $^{232}Th$ and $^{40}K$, respectively. From the MDA results, the detector sensitivity was not good enough with the counting time constrained to one week.

## 4. Conclusion

To have a good understanding of the radiogenic backgrounds, especially the radiogenic gamma rays from the PMTs that are used in the LUX and XENON100 detectors, we have designed a Ge-based well detector and a R11410MOD PMT in a Geant4-based Monte Carlo simulation. Two independent simulations were conducted for studying the detector response to the signal from the PMT and the detector response to the background from the copper boxes that are around the Ge planar detectors. In these two simulations, the detector performance including three types of detector efficiency, energy resolution and the Minimum Detectable Activity (MDA)
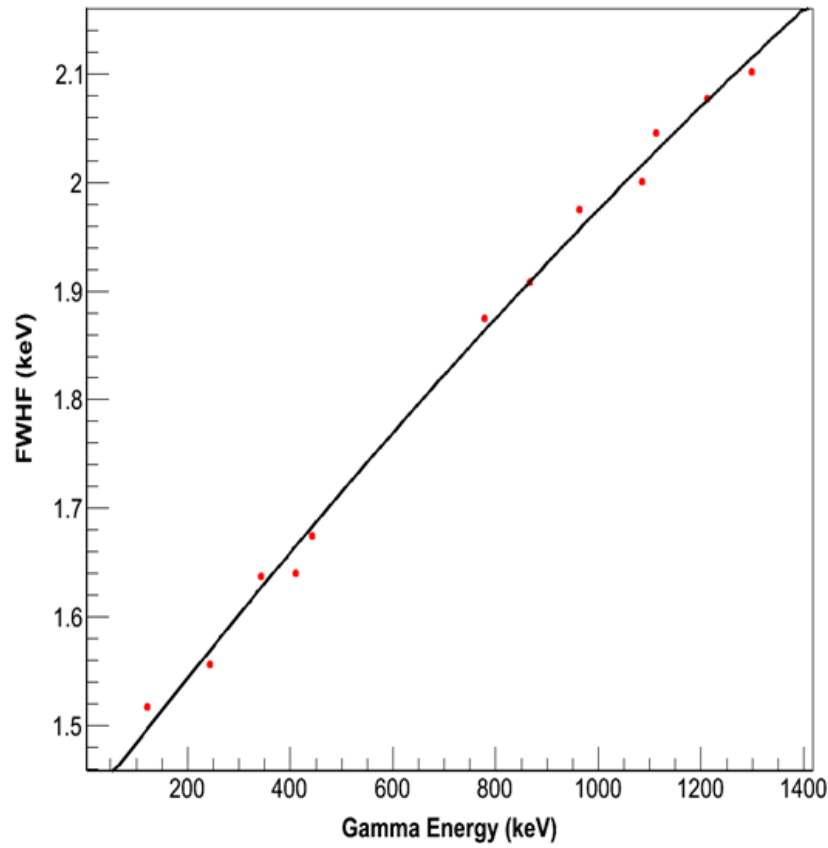
**Figure 2.** Energy resolution (FWHM) vesus the energy of gamma rays.

**Table 6.** $FWHM$ and $MDA$ for each selected gamma ray from $^{238}U$ decay chain.

| Raduinuclide | $E_\gamma$ (keV) | $FWHM$ (keV) | $\Delta T$ (s) | $N_b$ | $MDA$ (mBq/kg) | $MDA$ (mBq/PMT) |
|---|---|---|---|---|---|---|
| $^{234}Th$ | 92 | 1.48 | 2.66E+10 | 14189 | 1.28E-02 | 6.32E-02 |
| $^{234}Pa$ | 1001 | 1.98 | 2.66E+10 | 1502 | 8.69E-03 | 4.30E-02 |
| $^{226}Ra$ | 186 | 1.54 | 2.66E+10 | 14020 | 3.61E-03 | 1.79E-02 |
| $^{214}Pb$ | 352 | 2.46 | 2.66E+10 | 69422 | 8.84E-04 | 4.38E-03 |
| | 295 | 2.34 | 2.66E+10 | 41708 | 1.26E-03 | 6.25E-03 |
| $^{214}Bi$ | 2204 | 1.6 | 2.66E+10 | 2823 | 3.12E-03 | 1.54E-02 |
| | 1847 | 1.64 | 2.66E+10 | 1813 | 3.33E-02 | 1.65E-01 |
| | 1764 | 2.04 | 2.66E+10 | 9719 | 1.68E-03 | 8.31E-03 |
| | 1120 | 2.32 | 2.66E+10 | 9145 | 3.20E-03 | 1.59E-02 |

have been studied. According to the simulation results, we can conclude that this proposed germanium well detector has the capability of being sensitive to the PMTs with radioactivity

**Table 7.** $FWHM$ and $MDA$ for each selected gamma ray from $^{232}Th$ decay chain.

| Raduinuclide | $E_\gamma$ (keV) | $FWHM$ (keV) | $\Delta T$ (s) | $N_b$ | $MDA$ (mBq/kg) | $MDA$ (mBq/PMT) |
|---|---|---|---|---|---|---|
| $^{228}Ac$ | 969 | 1.96 | 1.11E+11 | 67922 | 5.69E-02 | 2.81E-01 |
|  | 911 | 1.94 | 1.11E+11 | 114699 | 3.18E-01 | 1.57E+00 |
|  | 338 | 1.62 | 1.11E+11 | 109630 | 2.88E-02 | 1.43E-01 |
| $^{228}Th$ | 84.4 | 1.48 | 1.11E+11 | 25738 | 3.78E-03 | 1.87E-02 |
| $^{224}Ra$ | 241 | 1.56 | 1.11E+11 | 53904 | 3.40E-03 | 1.68E-02 |
| $^{212}Pb$ | 239 | 1.56 | 1.11E+11 | 8374 | 5.17E-03 | 2.56E-02 |
| $^{212}Bi$ | 727 | 1.84 | 1.11E+11 | 38301 | 4.61E-01 | 2.28E+00 |
| $^{208}Ti$ | 583 | 1.76 | 1.11E+11 | 129893 | 2.18E-02 | 1.08E-01 |

**Table 8.** $FWHM$ and $MDA$ for the selected gamma ray from $^{40}K$ decay chain.

| Raduinuclide | $E_\gamma$ (keV) | $FWHM$ (keV) | $\Delta T$ (s) | $N_b$ | $MDA$ (mBq/kg) | $MDA$ (mBq/PMT) |
|---|---|---|---|---|---|---|
| $^{40}K$ | 1461 | 2.18 | 1.98E+10 | 29794 | 2.34E-02 | 1.16E-01 |

around 0.01 ppb.

## References

[1] Akerib D S *et al.* (LUX Collarboration) 2013 *NIM A*, Volume 703, p. 1-6. arXiv:1205.2272v2.
[2] Aprile E *et al.* (XENON100 Collaboration) 2012 *Phys. Rev. Lett.* **109** 181301 arXiv:1207.5988.
[3] Akerib D S *et al.* (LUX Collaboration) 2013 *Phys. Rev. Lett.* **112** 091303 arXiv:1310.8214.
[4] LZ Collaboration, http://lz.lbl.gov/.
[5] Aprile E *et al.*(XENON1T Collaboration) 2012, arXiv:1206.6288.
[6] Refer to: http://www-eng.lbl.gov/ shuman/NEXT/MATERIALS&COMPONENTS/PMT/PMT_R11410MOD_2010-0323.pdf.
[7] Heusser G *et al.*, Radioactivity in the Environment, DOI: 10.1016/S1569-4860 (05) 08039-3.
[8] Refer to http://www.lanl.gov/orgs/n/n1/panda/00326398.pdf.
[9] Refer to http://hepwww.rl.ac.uk/ukdmc/radioactivity/U238_chain/U238_chain.html.
[10] Refer to http://hepwww.rl.ac.uk/ukdmc/radioactivity/Th_chain/Th_chain.html.
[11] Currie LA 1968 *Analytical Chemistry* 40 (**3**) 587-593.
[12] Abhigyan A, Resolution and efficiency of high purity germanium, Refer to: http://www.academia.edu/4191151/Resolution_and_Efficiency_of_High_Purity_Germanium_Detector.